Geophysical Prospecting, 2000, **48**, 631–645

Diffraction problems of 3D seismic imaging

B.R. Zavalishin[1]

Abstract

Migration is essential to seismic imaging. It is carried out by backward extrapolation of the wavefield registered on the observation surface. The quality of images depends on the accuracy of the wavefield reconstruction at interior subsurface points. From the theory based on the exact solution of the scalar wave equation it is known that, for accurate wave extrapolation, data must be obtained from an infinite observation surface. Limiting of migration apertures, which is inevitable in practice, leads to artefacts in extrapolated fields. The distortion they cause in 2D and 3D imaging is different. In 2D migration, the artefacts known as truncation effects are much weaker than the signals being extrapolated and for this reason attract no special attention. In 3D migration, diffractions caused by an aperture edge are stronger and may create serious problems. For a circular aperture, their amplitudes are comparable to the amplitudes of the signals themselves. The study of aperture diffractions is intended to help in the search for ways of either suppressing them efficiently or deliberately utilizing them in order to improve imaging.

In optics, diffractions by an aperture play a constructive role in image making. This research shows that the same may take place in seismic imaging.

Introduction

Imaging in reflection seismology is based on backward wavefield extrapolation (migration). From Kirchhoff's solution of the scalar wave equation it is known that the correct solution of the wave extrapolation problem is only possible using data from an infinite observation surface. The limitation of a surface by an aperture of any shape or size results in the appearance of edge diffractions accompanying the extrapolation of each wave. In 2D migration these truncation effects are weak and after additional attenuation by high-fold stacking, they create no serious problems (see, for example, Al-Yahya 1989). In 3D the situation is different for two reasons: diffractions by an aperture are stronger and the stacking fold is not ordinarily so high. In essence the situation with 3D imaging is similar to the situation in optics, where diffraction by an

Paper presented at the 59th EAGE Conference – Geophysical Division, Geneva, Switzerland, May 1997. Received April 1998, revision accepted December 1999.

[1] Russian State University of Oil and Gas, 65 Leninsky prospekt, Moscow 117296, Russia.

aperture plays a fundamental role. In seismology, as in optics, this role may be constructive or destructive, and for this reason is worth studying.

In optics (Pohl 1963; Born and Wolf 1964), images of continuous objects are created by a small light spot (an Airy spot) originating from the constructive interference of the wave passing through an aperture with the waves diffracted by its rim. Natural conditions for constructive interference exist in the far (Fraunhofer) zone. The same conditions are artificially created by a lens in the vicinity of its focal point, which is why focusing is an essential part of imaging in optics.

In seismology, backward extrapolation is designed to reconstruct waves existing at discontinuities inside the geological medium. Whether or not such a reconstruction leads to focusing depends on the type of discontinuity. It is evident that the backward extrapolated wave originally scattered by a localized intrusion should be focused on it, while the reflection from a flat boundary should not, because the original reflected wave was not focused there. Absence of focusing indicates that the extrapolated wave and the aperture diffractions accompanying it do not interfere constructively. The consequences of this for 2D and 3D imaging are different and in the latter case depend significantly on the aperture shape and dimensions.

Diffractions in migration and focusing

Extrapolation (migration) from an infinite observation surface enables the reconstruction of propagating waves at interior subsurface points. Limitation of the aperture leads to the appearance of non-existent diffracted waves that may be treated as noise. Whether or not this noise pollutes images depends on the type of wave being extrapolated and the instant in time selected for imaging. Figure 1 demonstrates these properties from a kinematic point of view. Consider migration of a common-shot seismogram when the earth model consists of either a plane reflector or a local discontinuity, both at the same depth z. Imagine also two cases: an infinite aperture (Fig. 1a) and a limited aperture (Figs 1b and c).

At the instant $t = z/v + \delta$, slightly exceeding the time of reflection or scattering, migration from an infinite aperture (Fig. 1a) restores the wavefronts of both propagating waves without any artefacts. When the aperture is limited (Fig. 1b), undesired wavefronts diffracted by the aperture edges appear in the extrapolated field. At the instant $t = z/v$, coinciding with the reflection (scattering) time, the wavefront of the extrapolated reflected wave is tangential to the reflector and the wavefront of the extrapolated scattered wave is focused on a point (Fig. 1c). Thus this is a suitable instant for mapping the extrapolated field to construct a seismic image. From Fig. 1c, it is clear that the imaging of different objects using a limited aperture does not provide equally favourable results. The image of a point scatterer, if such a geological object were physically possible (Zavalishin 1994), would be excellent and free from noise. On the other hand, the image of a reflecting boundary cannot be free from diffraction noise above it. Because *reflection seismic* deals primarily with *reflected* waves, the problem of diffraction noise on seismic images should not be neglected.

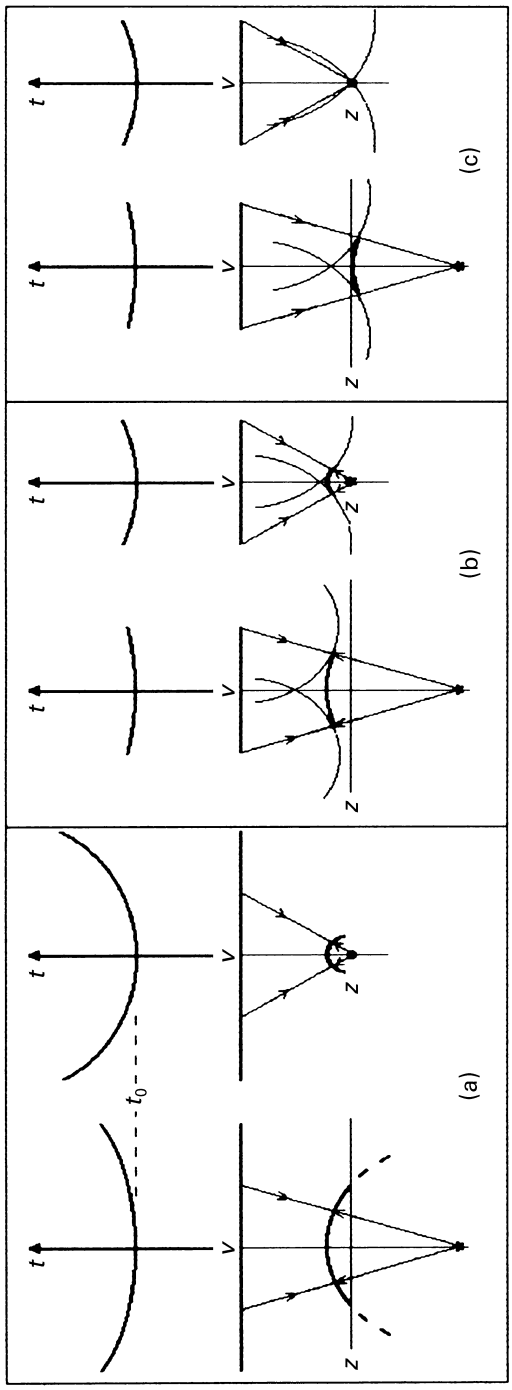

Figure 1. Imaging of a reflector and a localized scatterer. (a) Migration from an infinite aperture reconstructs wavefronts of reflected or scattered waves without artefacts. (b) Limitation of an aperture leads to the appearance of diffracted wavefronts centred at the aperture edges. (c, right) At the moment of imaging the scattered wavefront is focused on a point. Diffracted wavefronts passing through the same point do not distort the image. (c, left) The image of a reflector taken at the same instant is polluted by diffraction wavefronts at shallower depths. In 2D migration they are known as truncation effects.

Figure 1 also demonstrates that the problem of diffraction noise on seismic images only exists when an extrapolated wave is not focused. In Fig. 1c (right), the focusing of the scattered wave occurs at the instant $t = z/v$ when the diffracted wavefronts pass through the same point without creating noise elsewhere on the vertical axis. Though not shown, it is obvious that the focusing of the reflected wave on the imaginary source point (Fig. 1c, left) would occur at the instant $t = 0$. The imaging at $t = z/v$ is associated with the so-called diffraction stack type of migration. Similarly, the imaging at $t = 0$ is associated with the reflection stack type of migration, which was suggested by Timoshin (1978), but has not found wide application in practice. The situation may change when a better understanding of different problems specific to 3D imaging is reached. Nevertheless, only the commonly accepted $t = z/v$ imaging concept (Claerbout 1985) is discussed here.

A simple 2D/3D diffraction relationship

The Kirchhoff-type solution of the migration problem is essentially described by summation of seismograms along hyperbolae assigned to each point in the imaging space. Consider a 2D common-shot seismogram along the x-direction containing one reflection from a horizontal boundary. Figure 2a shows the time–distance curve together with three stacking hyperbolae. Migration of this seismogram into points 1, 2 and 3 on the z-axis presumes summation along the corresponding hyperbolae. Hyperbola 1 stacks signals over the zone tangential to the reflection and sums them at point 1 on the reflector, thus constructing the desired image. It is evident that the

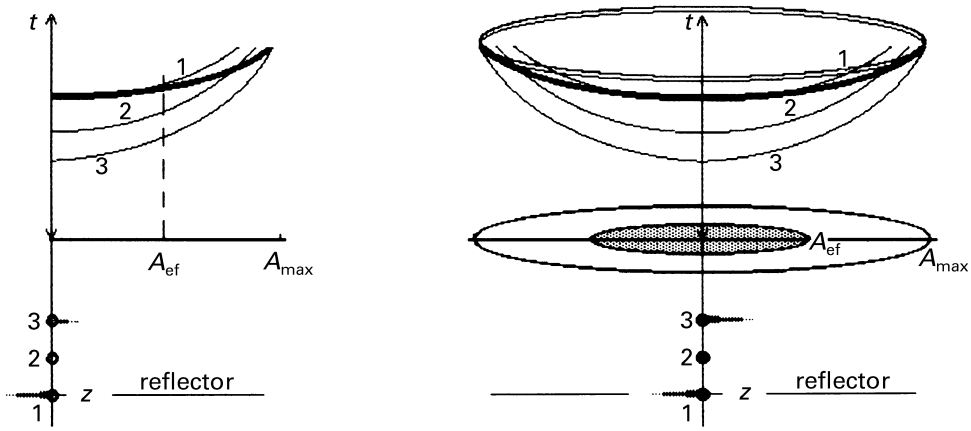

Figure 2. Schematic diffraction-stacking migration of the reflected wavefront: (a) on an ordinary (x,t) common-shot seismogram and (b) on a circular (x,y,t) common-shot seismogram. Note that diffraction noise 3 is much stronger in 3D migration (b).

amplitude of the migrated signal S_{2D} should somehow depend on the tangential zone length $A_{ef.}$ This will be discussed below.

All hyperbolae crossing and stacking positive and negative phases along the full length of the reflected signal, such as hyperbola 2, should theoretically give zero amplitude at the corresponding point on the z-axis (Zavalishin 1975). For 2D extrapolation and for approximate algorithms it is not exactly zero, but it is negligibly small.

Due to the wavefield discontinuity at the end of the spread A_{max}, hyperbola 3 does not cross and stack along the full length of the reflected signal. For this reason it gives a non-zero amplitude at the corresponding point on the z-axis.

To illustrate the above discussion, the model reflection seismogram ($z = 1.5$ km, $v = 2$ km/s, $\Delta x = 25$ m, $A_{max} = 1$ km) was time-migrated to zero offset using the simplest diffraction stack algorithm (Fig. 3). Truncation noise similar to that marked N_{2D} is often seen in practice on migrated single-fold gathers but is efficiently attenuated by high-fold stacking (see, for example, Al-Yahya 1989). The relative

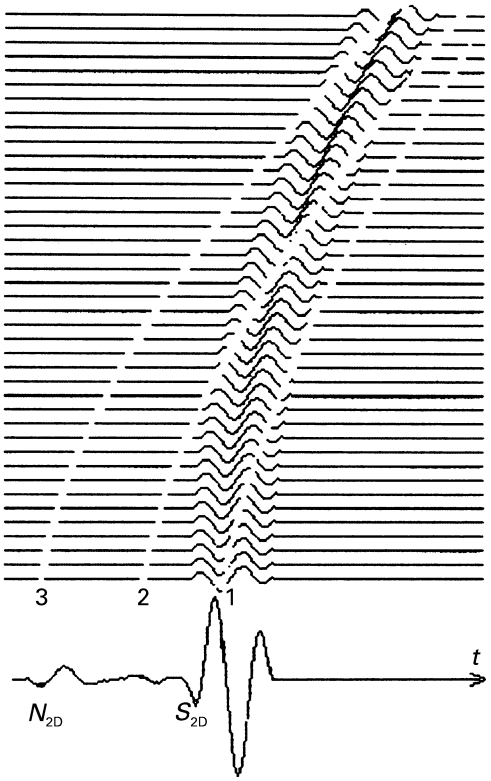

Figure 3. Diffraction-stacking time migration of the reflection on a model common-shot seismogram. Stacking hyperbolae are shown schematically. The real differences in their shape are less distinct.

strength of this noise in 2D is not high. In Fig. 3, the ratio S_{2D}/N_{2D} is equal to 8.33. To demonstrate that in the 3D case the situation would be worse, consider the transformation of an ordinary (x,t) common-shot seismogram into an (x,y,t) circular seismogram.

This transformation can be carried out by rotating the 2D seismogram around the vertical axis (Fig. 2b). Although the circular seismogram is not very common in practice, it is used here because it suggests a simple explanation. After migration of the 3D seismogram, the amplitudes of the signal (1) and noise (3) increase in different proportions. The amplitude of the signal S_{2D} (Fig. 3) is increased by a factor of πA_{ef}^2, which is equal to the circular tangential zone area (Fig. 2b), while the amplitude of the noise N_{2D} is increased by a factor of $2\pi A_{max}$, which is equal to the circumference of the full aperture, so that

$$S_{3D} = \pi A_{ef}^2 S_{2D}, N_{3D} = 2\pi A_{max} N_{2D}.$$

Accordingly, the signal-to-noise ratio of 3D migration becomes smaller in comparison with 2D migration, so that

$$(S/N)_{3D} = \frac{A_{ef}^2}{2A_{max}}(S/N)_{2D}, \quad (1)$$

because in practice an aperture size A_{max} is usually bigger than 1 km and a tangential zone A_{ef} is smaller.

The simplicity of the idea used to obtain (1) may appear to be unconvincing. The numerical experiments described below demonstrate both the verification of the formula and the evaluation of A_{ef}. The latter is important not only for the problem under consideration here, but for seismic imaging in general.

2D migration model experiments

Consider the depth migration of the seismogram, shown in Fig. 4a, to the point on the horizontal reflector ($z = 1.5$ km, $v = 2$ km/s) beneath the source. Results of migration with gradually increasing apertures are shown in Fig. 4b. A simple diffraction stack algorithm was used and each migrated trace was placed under the aperture edge in Fig. 4a. This experiment reveals the controversial role of diffraction (truncation effect) in the extrapolated field and thus in the image. When the aperture is small, diffraction noise interferes significantly with the extrapolated reflection. Such interference yields a wavelet with shape and duration similar to the signal on the seismogram. This occurs because the hyperbola d (Fig. 4a) stacks only reflected signals with a nearly equal phase. With bigger apertures the signal and noise interference results in noticeable local amplification of the migrated wavelet. It still resembles the original signal shape but becomes longer in time. A further expansion of the aperture leads to distortion of the wavelet until finally it comes apart, providing complete temporal resolution of the signal and diffraction noise. This occurs when the aperture size is equal to A (Fig. 4a), corresponding to the point where the stacking

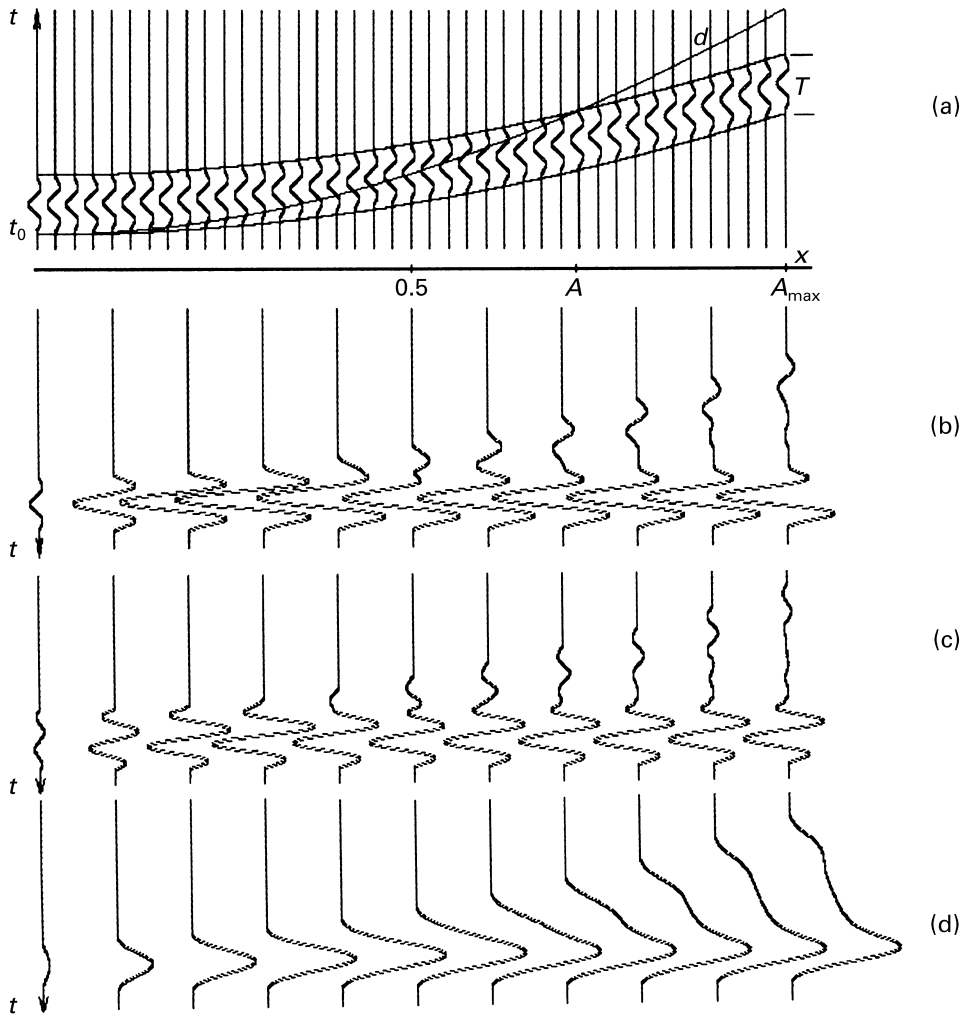

Figure 4. Depth migration of the common-shot seismogram (a) to the reflector point beneath the shot. *d* indicates the stacking hyperbola corresponding to this point. The aperture is gradually increased. Each migrated trace is placed beneath the aperture edge. The reflection on the seismogram was represented by: (b) a symmetric Ricker pulse; (c) its derivative; (d) their envelope.

hyperbola *d* crosses the rear wavefront of the reflected wave. For greater aperture sizes, the reconstructed signal does not change, which makes it easy to evaluate the signal-to-diffraction-noise ratio needed later to verify (1). Peak amplitudes or (Hilbert-defined) envelopes may serve this purpose. Both were used in this research and they produced similar results. Note that the migrated signal shape differs from that on the seismogram (Ricker pulse). This is not only because of the simplification

of the algorithm but also because the 2D extrapolation procedure is not capable of restoring a signal accurately in any case.

Up to now A_{ef} was defined only schematically as the tangential zone of the reflection and the stacking hyperbolae (Fig. 2). It may represent some aperture size responsible for the effective restoration of the reflected signal as a whole or any of its attributes. Thus it depends on the selection of a criterion. When complete restoration of a signal as a whole is the aim and the existence of aperture diffractions is neglected, the effective aperture size is $A_{ef} = A$ (Fig. 4a). Schleicher *et al.* (1997) called it the minimum aperture (A_{min}). However, in such a case the migrated signal is immediately followed by truncation (diffraction) noise (see Figs 4b and c here and Fig. 8c of Schleicher *et al.* (1997)). This diffraction noise, accompanying a strong reflection, may cause problems for the imaging of its weaker neighbours at shallower depths. It will be shown (Figs 6b and c) that in 3D migration this noise is much stronger and is unacceptable under any circumstances.

The physical meaning of A_{ef} in (1) is different. It is intended to provide only exact restoration of the signal amplitude ignoring its duration and shape. Such a criterion suggests the existence of a limit, after which further expansion of the aperture size cannot cause changes in the extrapolated signal amplitude. The Hilbert-defined amplitude of a signal does not depend on its frequency content because the same envelope may relate to a variety of signal shapes. From this it should follow that an aperture size responsible for the exact reconstruction of the true signal amplitude should not depend on frequency. To verify this assumption, the above experiment was repeated after replacing the symmetric Ricker pulse on the seismogram with its derivative. This guaranteed that the new signal had the same duration but a different frequency content. The results are shown in Fig. 4c. Note that all comments about Fig. 4b are also applicable here. To exclude the possibility of the frequency content influencing the results, a migration was performed after transformation of the signals on the seismogram into envelopes. It should be clear that the shape of the envelope was the same for both signals. The results are shown in Fig. 4d. Note that the amplitude of the migrated envelope increases gradually without local amplification at smaller apertures, which was seen for the signals.

To make the analysis of amplitudes more convenient, the graphs of the normalized amplitude as a function of the aperture size are plotted in Fig. 5. The same notations (b, c, d) corresponding to the situations in Fig. 4 are used for their identification. All three graphs show the same size after which further expansion of an aperture causes no changes in the amplitude of the extrapolated signal. It proves that the effective aperture size A_{ef}, corresponding to the criterion formulated above, does not depend on frequency. The experiment also shows that the aperture size enabling maximum amplification of the migrated wavelet depends on the signal shape and thus on frequency.

3D migration

Instead of similarly migrating a 3D seismogram with an inaccurate diffraction stack

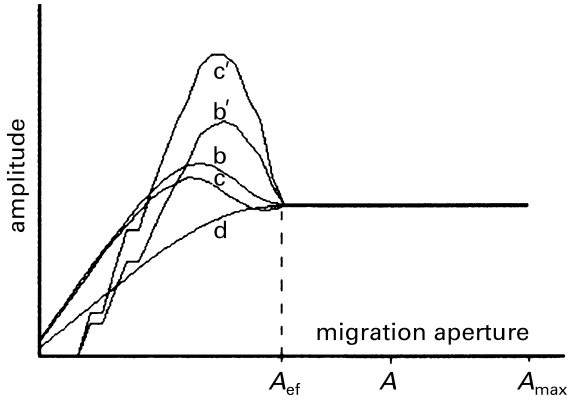

Figure 5. Graphs of the normalized maximum amplitude on migrated traces of Fig. 4 and Fig. 6 as a function of the migration aperture size.

algorithm, the exact solution of the backward extrapolation problem can be used (see Appendix). It describes explicitly the migrated scalar wavefield at any point on the vertical axis of a circular aperture. For the same point on the horizontal reflector at z (Fig. 2b), the solution is given by

$$u_z(t) = \frac{f\left(t - \frac{z}{v}\right)}{z} - \frac{f\left(t - \frac{\rho - r}{v}\right)}{2(\rho - r)}\left(\frac{2z}{\rho} + \frac{z}{r}\right), \tag{2}$$

where $f(t)$ is the signal shape on a common-shot seismogram. For other notations see Fig. 7. Equation (2) defines explicitly both the signal (the first term) and the aperture diffraction (the second term) in the extrapolated field. Because the shape of both is the same, the signal-to-noise relation is easy to calculate. It depends only on the geometrical factors: depth and aperture size. The results of migration with gradually increasing apertures calculated using (2) are shown in Fig. 6. Again the symmetric Ricker pulse and its derivative (Figs 6b and c, respectively) were used as reflected signals and each migrated trace was placed beneath the corresponding aperture edge in Fig. 6a. The shadowed zone represents the effective aperture size A_{ef} depicted in Fig. 5. Graphs of the normalized amplitude as a function of the aperture size are added to Fig. 5, denoted by b′ and c′. They support the selection of A_{ef} and show much stronger amplification of wavelets migrated with smaller apertures. The latter is explained by the fact that the amplitudes of diffractions are much higher in 3D. This is obvious from comparison of Figs 4 and 6.

Verification of equation (1)

All the data necessary to verify (1) have now been obtained. For practical purposes it is convenient to select $A_{max} = 1$ km. The signal-to-noise ratios $(S/N)_{3D}$, calculated from (2) and measured on the rightmost traces of Figs 6b and c, are both equal to

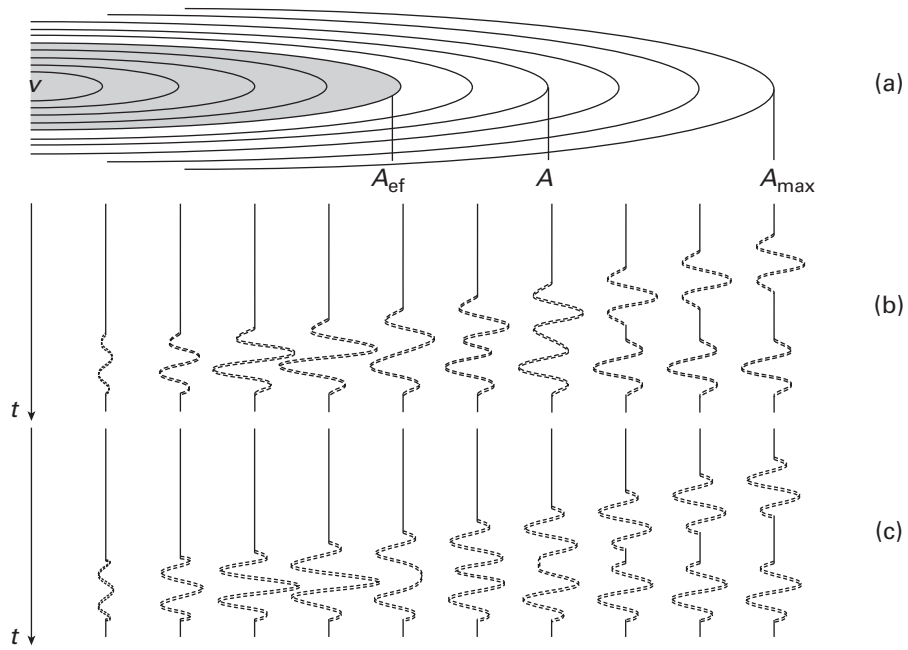

Figure 6. Depth migration of the reflection from the circular aperture of variable radius (a) into the reflector point on the z-axis using equation (2). The wave function was represented by: (b) a symmetric Ricker pulse; (c) its derivative. Compare with Fig. 4 and note that the diffraction noise has become much stronger.

1.02. For the 2D migration in Fig. 4, a similar evaluation can be performed. We obtain two values for $(S/N)_{2D}$: 7.14 for the Ricker pulse (Fig. 4b) and 8.33 for its derivative (Fig. 4c). The latter should be more accurate because migration algorithms such as that used here represent high-frequency approximations to the solution of the wave equation. With the values above, (1) yields $A_{ef} = 0.49$ km; the same value is found for A_{ef} from Fig. 5.

Physical explanation

It is obvious that both A and A_{ef} somehow depend on signal duration, and if the seismic signal were a spike of zero duration ($T = 0$), both would be equal to zero. The nature of this dependence for $T \neq 0$ is easier to reveal for a process that is physically possible. This is not the case for backward wavefield extrapolation. Fortunately, the aperture-size determination problem is similar to the problem of reflecting-area evaluation (Zavalishin 1975, 1981; Knapp 1991; Bruhl, Vermeer and Kiehn 1996). The latter is easier to understand because it can be formulated as a forward extrapolation problem, where the Huygens–Fresnel principle is helpful. At point S on the observation surface (Fig. 7), the reflection arrives at $t_0 = 2z/v = O_1S/v$ and lasts

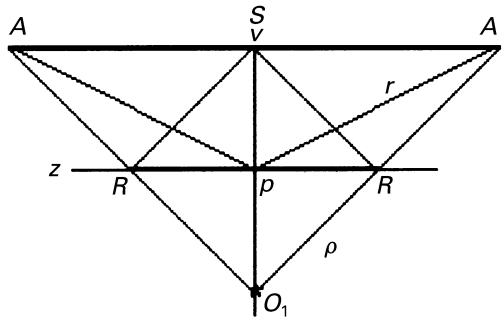

Figure 7. Geometry of forward and backward extrapolation problems. To construct a signal of given duration at S, the portion RR of the reflector is required. To reconstruct a signal of the same duration at P, the aperture size AA is required.

for time T. With the image source at O_1, the reflected signal at S may be considered to be created by constructive interference of Huygens waves coming from virtual point sources distributed along the reflector. At the same time, from the causality principle, it is clear that not all of these virtual waves can participate in the construction of the signal. Those from distant points on the reflector reach S after disturbance is known to be over. Therefore, a fixed duration of the signal limits the portion (RR) of the boundary contributing to the reflected signal construction. It also means that Huygens waves coming from outside this portion interfere at S destructively. This condition is expressed by the equation,

$$t_0 + T = (O_1R + RS)/v = \rho/v, \tag{3}$$

which geometrically leads to the expression,

$$R = \sqrt{vT(z + vT/4)}, \tag{4}$$

where $R = RR/2$. If T is small, so that $vT/4 < < z$,

$$R \approx \sqrt{vTz}. \tag{4a}$$

This simple way of obtaining these formulae, originally derived by Zavalishin (1975) as a result of a more complicated analysis, is shown here in order to define similarly an aperture size $A = AA/2$ (Fig. 7), necessary for exact restoration of a signal at point P on the boundary.

At boundary point P, the backward extrapolated wave arrives at $t_0/2 = z/v$ and lasts for time T. A fixed arrival time and limited duration of the backward extrapolated signal make it impossible for Huygens waves arriving from outside AA to contribute to the signal reconstruction. This condition is ruled by the equation,

$$z - vT = O_1A - AP = \rho - r = \sqrt{4z^2 + A^2} - \sqrt{z^2 + A^2}. \tag{5}$$

After first-order expansion of the radicals (Fresnel approximation), it is easy to obtain

$$A \approx 2\sqrt{vTz}. \tag{6}$$

The physical explanation of the above formulae is as simple as the formulae themselves. For the accurate construction of a reflected signal at S or its reconstruction at P, boundary conditions must not be changed within radii given by (4a) on the reflector and (6) on the observation surface, respectively. Any change leads to diffraction that will inevitably distort the signal. Causality and Huygens–Fresnel principles allow the prediction of the diffraction arrival time from a point where the boundary conditions changed. For example, if an aperture is limited by A (equation (6)), diffraction appears in the extrapolated field at $t_0/2 - T$. It immediately follows the undistorted signal (see Figs 6b and c for 3D; Figs 4b and c and Fig. 8c in Schleicher *et al.* 1997 for 2D). The same approach makes it easy to define the aperture dimension assumed to provide the restoration of the exact signal amplitude in the extrapolated field. As the amplitude of a signal can be properly defined with the help of its envelope maximum, diffraction may take place at the instant this maximum is reconstructed. If the time of the envelope maximum is τ, it should replace T in (6). For signals used in the above experiments $\tau = T/2 = 0.02$ s. With this value (6) gives $A_{\text{ef}} = 0.49$, coinciding with the dimension already determined experimentally (Fig. 5) and using (1).

From (2) it can be predicted that the maximum local amplification of the extrapolated (migrated) wavelet should occur when the first phase of the diffraction overlaps the second phase of the signal. It occurs when the time delay of the diffraction is equal to half of the apparent period of $f(t)$. Substituting this value in (6) instead of T, we obtain the aperture size that is most efficient for practical migration and imaging because insignificant distortion of the signal is compensated by its noticeable amplification. In this case diffraction by the aperture plays a constructive role as in most optical appliances. It is obvious that this dimension coincides with the first Fresnel zone for the backward extrapolation of the predominant harmonic.

A circular aperture is not very common in 3D practice. It is used here because of the relative simplicity of the analysis caused by the fact that it produces well-focused diffractions on the axis. With any other aperture shape or/and tapering, they become dispersed and weaken. Unfortunately, in 3D they are hardly ever weak enough to be neglected. Evaluations based on the work of Zavalishin (1981) show that if a circular aperture is replaced by the circumscribed square, the amplitude of diffraction will be about 0.8 of that for the circle. The amplitude of a diffraction by one edge (half-plane) is about 0.2. In a common case, diffraction by a rectangular aperture consists of four pulses, each of amplitude 0.2, which may randomly attenuate or amplify each other, thus creating apparently irregular noise. This is what Gardner and Canning (1994) and Canning and Gardner (1996) may have unintentionally demonstrated by their experiment. They showed that 3D images are much noisier than 2D (regular

zero-azimuth) images. Revealing a problem is often more important than solving it. One possible explanation of the phenomenon is suggested above.

A circular aperture is perfect only for imaging of horizontal reflectors. It is evident that, for a dipping reflector and/or migration along an inclined ray, the ideal aperture should be elliptical, replicating the Fresnel zone. In this case all discussions and results related to the circular aperture remain valid. Practical questions on the aperture dimensions and positioning on 3D data sets are discussed separately (Zavalishin and Parasyna 1999).

Conclusions

Aperture diffractions in 3D migration are much stronger than truncation effects in 2D migration. Diffractions accompany the extrapolation of each reflection. Depending on the aperture size they disrupt either the signal being extrapolated or neighbouring reflections from shallower boundaries. The theory of wave extrapolation from limited apertures excludes the possibility of their efficient elimination in common cases. Tapering will disperse aperture diffractions into irregular and weaker-looking noise but it inevitably results in distortion of the signals themselves. This makes any efforts to suppress diffractions in the process of migration of any single-fold data set highly controversial. Once it is accepted that diffraction is unavoidable and exact (i.e. with no noise at all) restoration of a signal is unattainable, a more practical solution becomes obvious. The aperture size should be of the order of the first Fresnel zone for the predominant harmonic. It should provide brighter and less distorted images in comparison with all other possibilities.

Acknowledgements

I am grateful to the Ministry of Natural Resources of the Russian Federation for partial financial support of this research and to the anonymous reviewer for comprehensive editing of the manuscript.

Appendix

Consider the problem of backward extrapolation of a wavefield emitted by the point source at z_0 and which is known inside the circular aperture s (Fig. 8). Clearly, z_0 may act as the image source for a horizontal reflector. At any point on the z-axis, the solution can be found (Zavalishin 1989) by evaluating the Kirchhoff integral,

$$u = \frac{1}{4\pi}\int_s \left\{ \frac{1}{r}\left[\frac{\partial F}{\partial n}\right] - \frac{1}{vr}\frac{\partial r}{\partial n}\left[\frac{\partial F}{\partial t}\right] - \frac{\partial}{\partial n}\left(\frac{1}{r}\right)[F] \right\} \mathrm{d}s. \tag{A1}$$

The known position of the source provides all necessary functions in explicit form for

a harmonic:

$$F = \frac{e^{j\omega t - jk\rho}}{\rho}, \frac{\partial F}{\partial n} = \frac{\partial F}{\partial \rho}\frac{\partial \rho}{\partial n} = -\frac{z_0}{\rho}\left(\frac{jk}{\rho} + \frac{1}{\rho^2}\right)e^{j\omega t - jk\rho}, \frac{\partial F}{\partial t}$$

$$= j\omega\frac{e^{j\omega t - jk\rho}}{\rho}, \frac{\partial r}{\partial n} = \frac{z}{r}, \frac{\partial \rho}{\partial n} = \frac{z_0}{\rho}, \frac{\partial}{\partial n}\left(\frac{1}{r}\right) = -\frac{z}{r^3},$$

where $\rho = \sqrt{x^2 + y^2 + z_0^2}, r = \sqrt{x^2 + y^2 + z^2}$, ω denotes frequency, $k = \omega/v$ denotes wave number and v denotes acoustic velocity. Square brackets denote the addition of jkr to the exponent. In polar coordinates $ds = RdRd\theta = rdrd\theta$. Points lying on the z-axis are independent of θ. After integration over this variable and omitting $e^{j\omega t}$ for simplicity, we obtain

$$u_z = \frac{1}{2}\int_z^{r_a}\left\{\frac{z}{r^2} - \frac{z_0}{\rho^2} - jk\left(\frac{z_0}{\rho} + \frac{z}{r}\right)\right\}\frac{e^{-jk(\rho - r)}}{\rho}dr, \tag{A2}$$

where $r_a = \sqrt{a^2 + z^2}$, a denotes the aperture radius. Since $\rho d\rho = rdr$, it is easy to check that

$$\frac{d}{dr}\left[-\frac{e^{-jk(\rho - r)}}{\rho - r}\left(\frac{z_0}{\rho} + \frac{z}{r}\right)\right] = \left\{\frac{z}{r^2} - \frac{z_0}{\rho^2} - jk\left(\frac{z_0}{\rho} + \frac{z}{r}\right)\right\}\frac{e^{-jk(\rho - r)}}{\rho}$$

and obtain the exact value of (A2) in the form

$$u_z = \frac{e^{-jk(z_0 - z)}}{z_0 - z} - \frac{e^{-jk(\rho_a - r_a)}}{2(\rho_a - r_a)}\left(\frac{z_0}{\rho_a} + \frac{z}{r_a}\right), \tag{A3}$$

where $\rho_a = \sqrt{a^2 + z_0^2}$. It shows that the backward extrapolated wavefield consists of two interfering waves: the original spherical wave and the wave diffracted by the

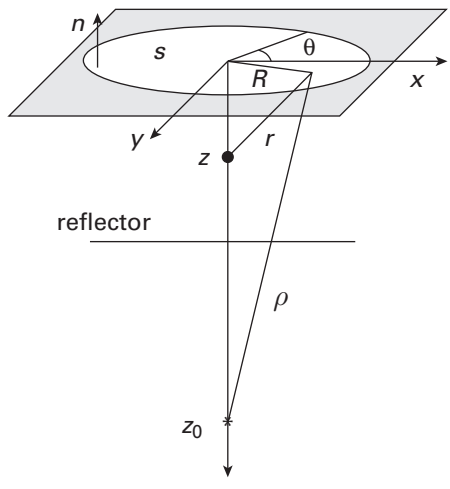

Figure 8. Geometry of backward extrapolation of a wavefield emitted by a point source at z_0.

aperture rim. At a distance from the observation surface both waves have nearly equal amplitudes. Note that the singularity at $z = z_0$ can be resolved using the L'Hopital rule. It leads to the result,

$$u_{z_0} = -\frac{\mathrm{j}k(\rho_a - z_0)}{\rho_a}, \tag{A4}$$

coinciding with the known Debye's solution (Sommerfeld 1964). Note also that Debye's solution is exact only at this point. Elsewhere it is accurate if the optical approximation is applicable (Born and Wolf 1964). Conversely, the solution (A3) is exact along the z-axis and for this reason is self-consistent: if $z = 0$ and $a \to \infty$, it restores the boundary condition assigned to this point at the start. If the harmonic is replaced with an arbitrary wave function, $F = f(t - \rho/v)/\rho$, the solution (A3) takes the form,

$$u_z = \frac{f\left(t - \frac{z_0 - z}{v}\right)}{z_0 - z} - \frac{f\left(t - \frac{\rho_a - r_a}{v}\right)}{2(\rho_a - r_a)}\left(\frac{z_0}{\rho_a} + \frac{z}{r_a}\right), \tag{A5}$$

used in the main text.

References

Al-Yahya K.M. 1989. Velocity analysis by iterative profile migration. *Geophysics* **54**, 718–729.

Born M.A. and Wolf E. 1964. *Principles of Optics*. Pergamon Press, Inc.

Bruhl M., Vermeer G.J.O. and Kiehn M. 1996. Fresnel zones for broadband data. *Geophysics* **61**, 600–604.

Canning A. and Gardner G.H.F. 1996. Another look at the question of azimuth. *Leading Edge* **15**, 821–823.

Claerbout J.F. 1985. *Imaging the Earth's Interior*. Blackwell Scientific Publications.

Gardner G.H.F. and Canning A. 1994. Effects of irregular sampling on 3D prestack migration. 64th SEG meeting, Los Angeles, USA, Expanded Abstracts, 1553–1556.

Knapp R.W. 1991. Fresnel zones in the light of broadband data. *Geophysics* **56**, 354–359.

Pohl R.W. 1963. *Optik und Atomphysik*. Springer-Verlag, Inc.

Schleicher J., Hubral P., Tygel M. and Jaya M. 1997. Minimum apertures and Fresnel zones in migration and demigration. *Geophysics* **62**, 183–194.

Sommerfeld A. 1964. *Optics*. Academic Press, Inc.

Timoshin Yu.V. 1978. *Seismic Pulse Holography*. Nedra (in Russian).

Zavalishin B.R. 1975. The size of the region that forms a reflected wave at a boundary. *Prikladnaya Geofizika* **77**, 67–74. Nedra (in Russian). (English translation: *Stanford Exploration Project Report no. 28*, Stanford University, 1981, pp. 345–353.)

Zavalishin B.R. 1981. Analysis of ideas on effective dimensions of the reflecting surface. *Prikladnaya Geofizika* **100**, 36–44. Nedra (in Russian).

Zavalishin B.R. 1989. Accuracy of focusing in seismic imaging. *Transactions (Doklady) of the USSR Academy of Sciences* **309**, 835–836 (in Russian).

Zavalishin B.R. 1994. Wave approach to seismic imaging. *Geofizika* **4**, 29–32 (published in both Russian and English).

Zavalishin B.R. and Parasyna V.S. 1999. Migration and imaging with the optimal aperture. 61st EAGE conference, Helsinki, Finland, Extended Abstracts, P-136.